Influence of changing temperature and upwelling intensity on Indian oil sardine (*Sardinella longiceps*) landings

Eli E. Holmes[1], Smitha B.R.[2], Nimit Kumar[3], Sourav Maity[3], David M. Checkley[4], Mark L. Wells[5], Vera L. Trainer[1]

1. Northwest Fisheries Science Center, NOAA, Seattle, WA.
2. Centre for Marine Living Resources and Ecology, MoES, Kochi, India.
3. Indian National Centre for Ocean Information Services, Hyderabad, India.
4. Scripps Institution of Oceanography, UC San Diego, San Diego, CA.
5. School of Marine Sciences, University of Maine, Orono, ME.

Running title: Modeling Indian oil sardine landings

Acknowledgements

We thank the U.S. National Marine Fisheries Service and the Indian Ministry of Earth Sciences for support of the the joint U.S.-Indian research project: “Collaboration on the Development of a Fisheries and Harmful Algal Bloom and Monitoring and Prediction System in Indian Seas” which jointly provided the financial support for the research visits. The visits took place at the Indian National Centre for Ocean Information Services (INCOIS) and Centre for Marine Living Resources and Ecology (CMLRE). We thank these institutes for their support during the research visits. We would also like to specifically acknowledge the support of Dr. S.S.C Shenoi (INCOIS), Dr. M. Sudhakar (CMLRE), Dr. N. Saravanane (CMRLE), Dr. Ned Cyr, Dr. Kevin Werner (NOAA) and Dr. Usha Varanasi for their support. The sardine landings data have been collected and analyzed by the Central Marine Fisheries Research Institute (Cochi, India) since the 1950s; we acknowledge the many researchers involved in collecting and maintaining this long-term data set.

Abstract

Commercial landings of sardine are known for strong year-to-year fluctuations. A key driver is thought to be environmental variability, to which small forage fish are especially sensitive. We examined the environmental drivers associated with landings fluctuations in the Indian oil sardine using a 32-year time series off Kerala state. Past research suggested a variety of influential variables: precipitation, upwelling intensity, ocean temperature (SST), chlorophyll density and large-scale coupled atmosphere–ocean phenomena (ENSO). Using the life-history of the Indian oil sardine, we developed hypotheses concerning how these environmental variables might affect landings and tested them using generalized additive models which allow non-linear response curves and dynamic linear models which allow time-varying responses. We found significant correlation for only two variables: upwelling intensity and the multi-year average nearshore SST. Both monsoon and post-monsoon landings were correlated with upwelling intensity in June-September. Upwelling intensity has both a positive effect (fueling higher food availability) and a negative effect at extreme intensity (bringing poorly oxygenated water to the surface). However, the most significant correlation (adjusted R^2 of 67.5%) was between the 2.5 year average nearshore SST and post-monsoon landings. The multi-year average SST also been identified as a predictor for Pacific sardine and southern African sardine fluctuations, suggesting that the average SST over the sardine life-span successfully captures a variety of factors which predict future abundance. The temperature in the Western Indian Ocean has been steadily increasing and the warming has been most extreme during the summer monsoon. Our work highlights that changes in sea temperature are likely affecting oil sardine landings but we found no evidence of effects of high temperature events but only low temperature events.

Keywords: Indian oil sardine, catch prediction, GAM modeling, climate, sea surface temperature, remote sensing, Southeastern Arabian Sea

Introduction

Environmental variability is known to be a key driver of population variability of small forage fish such as sardines, anchovy and herring (Alheit & Hagen, 1997; Checkley et al., 2017; Cury et al., 2000). In particular, ocean temperature and upwelling dynamics, along with density-dependent feedback, have been identified as important in affecting recruitment success and biomass of European and Pacific sardines (*Sardina pilchardus* and *Sardinops sagax*) (Alheit et al., 2012; Garza-Gil et al., 2015; Jacobson & MacCall, 1995; Lindegren & Checkley, 2012; Lindegren et al., 2013; Rykaczewski & Checkley, 2008). Like other sardines, the Indian oil sardine (*Sardinella longiceps* Valenciennes, 1847) shows strong inter-annual fluctuations and larger decadal booms and busts. The Indian oil sardine offers an instructive case study to investigate the effects of environmental variability, particularly temperature and upwelling dynamics, as they occupy an ocean system that is warmer than that occupied by other sardines and have a strong seasonal cycle driven by the Indian summer monsoon.

The Indian oil sardine is one of the most commercially important fish resources along the southwest coast of India (Figure 1) and historically has comprised approximately 25% of the marine catch in the Indian fisheries (Vivekanandan et al., 2003). Landings of the Indian oil sardine are highly seasonal, peaking after the summer monsoon period in October-December and reaching a nadir in spring before the summer monsoon in April-June (Figure 2). At the same time, the landings of this small pelagic finfish are highly variable from year to year. Small pelagics are well known to exhibit high variability in biomass due to the effects of environmental conditions on survival and recruitment, but in this fishery, environmental conditions also affect exposure of sardines to the fishery. Until recently, the Indian oil sardine fishery was artisanal and based on small human or low powered boats with no refrigeration. The fishery was confined to nearshore waters, and thus migration of sardines in and out of the coastal zone greatly affected exposure to the fishery and hence landings.

Researchers have examined a variety of environmental variables for their correlation with landings of the Indian oil sardine. Precipitation during the monsoon and the day of the monsoon arrival are thought to act as either a direct or indirect cue for spawning (Antony Raja, 1969, 1974; Jayaprakash, 2002; Murty & Edelman, 1966; Pitchaikani & Lipton, 2012; Srinath, 1998; Xu & Boyce, 2009). Although many studies have looked for and some have found correlations between precipitation and landings, the reported relationships are positive in some studies and negative in others (Madhupratap et al., 1994). Researchers have also looked for and found correlations with various metrics of upwelling intensity (Jayaprakash, 2002; Longhurst

& Wooster, 1990; Madhupratap et al., 1994; Murty & Edelman, 1966; Srinath, 1998; Thara, 2011), with direct measures of productivity such as nearshore zooplankton and phytoplankton abundance (George et al., 2012; Madhupratap et al., 1994; Menon et al., 2019; Nair, 1952; Nair & Subrahmanyan, 1955; Piontkovski et al., 2015; Pitchaikani & Lipton, 2012), and with near-shore sea surface temperature (SST) (Annigeri, 1969; Pillai, 1991; Prabhu & Dhulkhed, 1970; Supraba et al., 2016). SST can affect both somatic growth rates and juvenile survival but in this system also can cause fish to move off-shore and away from the shore-based fishery. The multi-year average sea temperature is postulated to have effects on recruitment and the survival of larval and juvenile sardines, which affect the later overall abundance (Checkley et al., 2017; Takasuka et al., 2007). The El Niño/Southern Oscillation (ENSO) has a cascading effect on all the aforementioned environmental parameters (SST, precipitation, upwelling) and correlations have been found between ENSO indices and sardine landings (Rohit et al., 2018; Supraba et al., 2016) and coastal anoxic events which affect sardines (Vallivattathillam et al., 2017).

In this paper, we study the utility of environmental covariates from remote sensing to explain year-to-year variability in oil sardine landings using a long-term time series of quarterly Indian oil sardine landings from the southwest coast of India. This time series is derived from a stratified sampling design that surveys the fishery landing sites along the southeast Indian coast and was first implemented in the 1950s (Srinath et al., 2005). The goal of the work presented here is to identify environmental covariates which can explain catch variability and improve the accuracy of short-term catch forecasts. Landings of oil sardines are determined by a combination of biomass, catchability, and effort. An auto-correlated catch model (ARIMA) can capture smooth changes in biomass and effort that cause landing variability, but the environmental variability adds a large component of year-to-year variability to small pelagic landings. In the Indian oil sardine system, catchability is strongly affected by the inshore versus offshore distribution of sardine. The fishery is restricted to the nearshore < 50 km offshore (Rohit et al., 2018) and when the sardines move offshore to spawn or to avoid hypoxic or excessive warm water, they are no longer available to the fishery. Thus, the environment has a strong impact on catchability. Biomass is driven by recruitment and survival are linked to environmental factors which determine food resources. The covariates which we study (Table 1) are linked to aspects of oil sardine life-history that are expected to affect catch via catchability or biomass. Covariates from remote sensing are the focus because they are available over a wide spatial extent at a daily and monthly resolution thus are practical for use in operational forecasts. A better understanding of how and whether remote sensing data explains variation in seasonal catch will support future efforts to use satellite data to improve catch forecasts.

Catch modeling versus biomass modeling

Modeling and forecasting landings data using statistical models fit to annual or seasonal catch time series has a long tradition in fisheries and has been applied to many species (Cohen & Stone, 1987; Farmer & Froeschke, 2015; Georgakarakos et al., 2006; Hanson et al., 2006; Lawer, 2016; Lloret et al., 2000; Mendelssohn, 1981; Nobel & Sathianandan, 1991; Prista et al., 2011; Stergiou & Christou, 1996), including oil sardines (Srinath, 1998; Venugopalan & Srinath, 1998). These models can be used to identity the variables correlated with catch fluctuations and can be used to provide landings forecasts which are useful for fishery managers and the fishing industry. An example of the former is using catch forecasts to set or give warnings of seasonal fishery closures if the forecasted catch is higher than the allowed catch limits (Farmer & Froeschke, 2015). An example of the latter is the annual Gulf and Atlantic menhaden forecast produced by NOAA Fisheries (Hanson et al., 2006; Schaaf et al., 1975). This multiple regression model has been used for the last 45 years to produce an annual forecast of menhaden landings, which is used for planning purposes by the industry, not only the fishers but also fish catch sellers and buyers, businesses which provide fisheries gear, and banks which provide financing (Hanson et al., 2006).

Unfortunately long-term biomass estimates are not possible for the Indian oil sardine. Length- or age-structured models (e.g. virtual population analysis) which produce biomass estimates are not possible due to the lack of effort and catch-at-age information for the fishery. The available long-term effort data are indirect (boat composition of the fishery at multi-year intervals) and estimates of number of trips or hours fishing are only available in a few recent years, and the data available are approximate given the vessel diversity of the fishery and sampling constraints. Nonetheless it is the case that the number and size of boats involved in the fishery has been increasing. Oil sardines are caught primarily by ring seines, which were introduced in the early 1980s. Ring seines of different sizes are used on both traditional small boats and on large mechanized ships (Das & Edwin, 2018). Since 1985, the ring seine fishery has expanded steadily in terms of horsepower, size of boats, and length of nets. There are concerns that over-fishing is a factor in the most recent oil sardine declines after 2015 (Kripa et al., 2018). Our base auto-correlated catch model is used to capture smooth trends due to changes due to steadily increasing effort.

For the purpose of our study, the assumption of a tight relationship between landings and abundance is not necessary. The objective is to understand what drives landings variability, whether it be due to abundance variability or due to exposure to the fishery (by being closer to shore). That said, Indian oil sardine landings are often assumed to reflect the total abundance for reasons specific to the species and the fishery (cf. Kripa et al., 2018). Historically, the fishery was artisanal: small boats with small motors, no refrigeration, and limited to the near shore. The ring seine was introduced in the 1980s, but widespread mechanization of the fleet is a very recent development. Fishers with small boats have limited ability to target the stock, at least not to the degree that landings remain constant as a stock declines. That pattern can be observed in a large, mobile, highly mechanized fleet. The fishery is unregulated, except for a brief closure during the monsoon months, thus the landings are not being affected by area closures and catch limits. Finally, the fishery is dispersed along the entire coastline rather than being focused from a few large ports. Again, for our objectives, it is not necessary that landings be a tight index of biomass, but there are many reasons to assume that this relationship is strong.

Study Area

Our analysis focuses on the Kerala coast (Figure 1) region of India, where the majority of the Indian oil sardines are landed and where oil sardines comprise ca. 40% of the marine fish catch (Srinath, 1998; Vivekanandan et al., 2003). This area is in the Southeast Arabian Sea (SEAS), one of world's major upwelling zones, with seasonal peaks in primary productivity driven by upwelling caused by winds during the Indian summer monsoon (Habeebrehman et al., 2008; Madhupratap et al., 2001) between June and September. Within the SEAS, the coastal zone off Kerala between 9°N to 13°N has especially intense upwelling due to the combined effects of wind stress and remote forcing (BR, 2010; BR et al., 2008). The result is a strong temperature differential between the near-shore and off-shore and high primary productivity and surface chlorophyll in this region during summer and early fall (BR, 2010; Chauhan et al., 2011; Habeebrehman et al., 2008; Jayaram et al., 2010; Madhupratap et al., 2001; Raghavan et al., 2010). The primary productivity peaks subside after September while mesozooplankton abundances increase and remain high in the post-monsoon period (Madhupratap et al., 2001).

Oil sardine life cycle and fishery

The Indian oil sardine fishery is restricted to the narrow strip of the western India continental shelf, within 20 km from the shore (Figure 1). The yearly cycle of the fishery begins at the start of spawning during June to July, corresponding with the onset of the southwest monsoon (Antony Raja, 1969; Chidambaram, 1950) and the initiation of strongly cooler nearshore SST due to upwelling (Figure 3). At this time, the mature fish migrate from offshore to coastal spawning areas, and the spawning begins during the southwest monsoon period when temperature, salinity and suitable food availability are conducive for larval survival (Chidambaram, 1950; Jayaprakash & Pillai, 2000; Krishnakumar et al., 2008; Murty & Edelman, 1966; Nair et al., 2016). Although peak spawning occurs in June to July, spawning continues into September (Antony Raja, 1969; Hornell, 1910; Hornell & Nayudu, 1923; Prabhu & Dhulkhed, 1970) and early- and late-spawning cohorts are evident in the length distributions of the 0-year fish. Spawning occurs in shallow waters outside of the traditional range of the fishery (Antony Raja, 1964), and after spawning the adults migrate closer to the coast and the spent fish become exposed to the fishery.

After eggs are spawned, they develop rapidly into larvae (Nair, 1959). The phytoplankton bloom that provide sardine larvae food is dependent upon nutrient influx from coastal upwelling and runoff from rivers during the summer monsoon and early fall. The blooms start in the south near the southern tip of India in June, increase in intensity and spread northward up the coast (BR, 2010). Variation in the bloom initiation time and intensity leads to changes in the food supply and to corresponding changes in the growth and survival of larvae and in the later recruitment of 0-year sardines into the fishery (George et al., 2012). Oil sardines grow rapidly during their first few months, and 0-year fish (40mm to 100mm) from early spawning appear in the catch in August and September in most years (Antony Raja, 1970; Nair et al., 2016). As the phytoplankton bloom spreads northward, the oil sardines follow, and the oil sardine fishery builds from south to north during the post-monsoon period. Oil sardines remain inshore feeding throughout the winter months, until March to May when the inshore waters warm considerably and sardines move off-shore to deeper waters (Chidambaram, 1950). Catches of sardines are correspondingly low during this time for all size classes. The age at first maturity occurs at approximately 150 mm size (Nair et al., 2016), which is reached within one year. When the summer monsoon returns, the oil sardine cycle begins anew.

Catches along the Kerala coast are high throughout the year except during quarter 2, April-June (Figure 2). The age-distribution caught by the fishery varies through the year. The fishery is closed during June to mid-July during the monsoon and peak spawning, and when it resumes in mid-July, it is first dominated by 1-2.5 year old mature fish (Antony Raja, 1969; Bensam, 1964; Nair et al., 2016). In August or September a spike of 0-year (40mm) juveniles from the June spawning typically appears in the catch (Antony Raja, 1969; Nair et al., 2016) and another spike of 0-year fish is sometimes seen in February from the late fall spawning (Prabhu & Dhulkhed, 1967, 1970). From October through June, the catch is dominated by fish from 120mm-180mm (Antony Raja, 1970; Nair et al., 2016; Prabhu & Dhulkhed, 1970) which is a mix of 0-year, 1-year and 2-year fish (Nair et al., 2016; Rohit et al., 2018).

Materials and Methods

Sardine landing data

Quarterly fish landing data have been collected by the Central Marine Fisheries Research Institute (CMFRI) in Kochi, India, since the early 1950s using a stratified multi-stage sample design (Srinath et al., 2005). The survey visits the fish landing centers along the entire southeast coast of India and samples the catch from the variety of boat types and gear types used in the coastal fishery. Landings estimates are available for all the coastal states, however we model the catch for the state of Kerala only, where the longest time series is available and the overwhelming majority of oil sardines are landed (Figure 2). The quarterly landings (metric tons) for oil sardine landed from all gears in Kerala were obtained from CMFRI reports (1956-1984) and online databases (1985-2015); see Appendix G for data sources. The quarterly landing data were log-transformed to stabilize the variance.

Remote sensing data

We analyzed monthly composites of the following environmental data derived from satellite data: sea surface temperature (SST), chlorophyll-a (CHL), upwelling (UPW), the Oceanic Niño Index (ONI), the Dipole Mode Index (DMI) and precipitation. The monthly time series and means of the covariates are shown in Figure 4.

For sea surface temperature, we used Advanced Very-High Resolution Radiometer (AVHRR) data, which provides accurate nearshore SST values. Although the ICOADS product provides SST values for earlier years, ICOADS does not provide accurate nearshore temperatures. For 1981 to 2003, we used the Pathfinder Version 5.2 product on a 0.0417 degree grid. These data were developed by the Group for High Resolution Sea Surface Temperature (GHRSST) and served by the US National Oceanographic Data Center. For 2004 to 2016, we used the NOAA CoastWatch SST products derived from NOAA's Polar

Operational Environmental Satellites (POES).

For chlorophyll-a, we used the chlorophyll-a products developed by the Ocean Biology Processing Group in the Ocean Ecology Laboratory at the NASA Goddard Space Flight Center. For 1997 to 2002, we used the chlorophyll-a 2014.0 Reprocessing (R2014.0) product from the Sea-viewing Wide Field-of-view Sensor (SeaWiFS) on the Orbview-2 satellite. These data are on a 0.1 degree grid. For 2003 to 2017, we used the MODIS-Aqua product on a 0.05 degree grid. These CHL data are taken from measurements by the Moderate Resolution Imaging Spectroradiometer (MODIS) on NASA's Aqua Spacecraft. The SST and CHL data were averaged across thirteen 1 degree by 1 degree boxes which roughly parallel the bathymetry (Figure 1). The SST and CHL satellite data were retrieved from NOAA remote-sensing data servers; see Appendix G for data sources and references.

For an index of coastal upwelling, we used three indices. The first was the sea-surface temperature differential between near shore and 3 degrees offshore based on the index described by Naidu et al. (1999) and BR et al. (2008). For SST, we used the remote sensing sea-surface temperature data sets described above. This SST-based upwelling index has been validated as a more reliable metric of upwelling off the coast of Kerala compared to wind-based upwelling indices (BR et al., 2008). The SST-based upwelling index and chlorophyll-a blooms are strongly correlated (Figure 3). The second index was simply average nearshore SST along the Kerala coasts (average of boxes 2-5 in Figure 1). The third index was the Bakun index based on wind stress. The index is computed from the the x- and y- components of Ekman Transport. See Appendix G for data sources and references.

Precipitation data were obtained from two different sources. The first was an estimate of the monthly precipitation (in mm) over Kerala from land-based rain gauges; these data are available from the Indian Institute of Tropical Meteorology and the data are available from the start of our landing data (1956). The second was a remote sensing precipitation product from the NOAA Global Precipitation Climatology Project. This provides estimates of precipitation over the ocean using a global 2.5 degree grid. We used the 2.5 by 2.5 degree box defined by latitude 8.75 to 11.25 and longitude 73.25 to 75.75 for the precipitation off the coast of Kerala. These data are available from 1979 forward. The land and nearshore ocean precipitation data are highly correlated (Appendix D). See Appendix G for the precipitation data repositories and references.

The Oceanic Niño Index (ONI) is a measure of the SST anomaly in the east-central Pacific and is a standard index of the El Niño/Southern Oscillation (ENSO) cycle. The ONI index is

3-month running mean of ERSST.v5 SST anomalies in the Niño 3.4 region, based on centered 30-year base periods updated every 5 years. The ONI was downloaded from the NOAA National Weather Service Climate Prediction Center. The Dipole Mode Index (DMI) is defined by the SSTA difference between the western Indian Ocean (10°S–10°N, 50°E–70°E) and the southeastern Indian Ocean (10°S–0°, 90°E–110°E). The DMI has been shown to predict anoxic events in our study area (Vallivattathillam et al., 2017). The DMI data were downloaded from the NOAA Earth System Research Laboratory. See Appendix G for the data servers where the ENSO data were downloaded and computation notes and references.

Hypotheses

Our statistical tests were structured around specific hypotheses (Table 1) concerning which remote sensing covariates in which months should correlate with landings in specific quarters. These hypotheses were based on biological information concerning how environmental conditions affect sardine survival and recruitment and affect exposure of Indian oil sardines to the coastal fishery. The Jul-Sep catch overlaps the summer monsoon and the main spawning months. This is also the quarter where small 0-year fish from early spawning often appear in the catch, sometimes in large numbers. Variables that affect or are correlated with movement of sardines inshore should be correlated with quarter 3 landings. In addition, pre-spawning (Mar-May) environmental conditions should be correlated with the spawning strength as adult oil sardines experience an acceleration of growth during this period along with egg development. The post-monsoon catch (Oct-May) is a mix of 0-year fish (less than 12 months old) and mature fish (greater than 12 months old). Variables that are correlated with spawning strength and larval and juvenile survival should correlate with the post-monsoon catch both in the current year and in future years, one to two years after.

Our hypotheses (Table 1) focus mainly on two drivers: upwelling and ocean temperature. We also test hypotheses concerning precipitation as this has historically been an environmental covariate considered to influence the timing of oil sardine landings. More recently, researchers have highlighted the influence of large-scale ocean processes, specifically the El Niño/Southern Oscillation, on sardine fluctuations; therefore we test the Ocean Niño Index (ONI) and Dipole Mode Index (DMI) also. Chlorophyll density is directly correlated with sardine food availability and chlorophyll fronts are known to influence sardine shoaling. However our chlorophyll time series is short (1997-2015) and the statistical power for testing correlation with landings is low. Tests of chlorophyll are shown in the appendices but are not the focus of our analyses.

Statistical models

We modeled the catches during the late-monsoon season (Jul-Sep) separately from the post-monsoon season (Oct-Mar). Thus, there is no seasonality in our catch time series as we analyzed a yearly time series of Jul-Sep catches separately from a yearly time series of Oct-Mar catches. We divided the catch in this way for biological and statistical reasons. Catch in Jul-Sep captures a mix of spawning age fish as it overlaps with the tail end of the spawning season, is affected by a fishery closure during the summer monsoon, and is periodically inflated by the appearance of small 0-year fish from early summer spawning. In addition, the covariates that affect the timing of spawning, movement of post-spawning mature fish inshore, and early egg and larval survival may be different than those that affect later growth, survival and shoaling that exposes fish to the inshore fishery. Analyzing catch and covariate time series without seasonality also had an important statistical benefit—we removed the problem of seasonality in the catch and covariates. The oil sardine life-cycle is seasonal and driven by the strong seasonality in this monsoon influenced system. A simple statistical model with quarters will explain much of the quarterly catch data since most of the yearly variability is due to seasonality and any environmental covariate with a similar seasonality will also show high correlation with the landings. Our goal was to explain year-to-year variability thus eliminating the confounding effect of seasonality in the data was important.

Preliminarily, we tested ARIMA models on both the Jul-Sep and Oct-Mar catch time series and found little support for auto-regressive errors (ARIMA models with a MA component) based on diagnostic tests of the residuals and model selection. The best supported ARIMA models were simple AR models ($x_t = bx_{t-1} + \varepsilon_t$). This lack of strong auto-correlation in residuals has been found in other studies that tested ARIMA models for forecasting small pelagic catch (Stergiou & Christou, 1996). We thus used AR-only models, however we tested both linear and non-linear models using generalized additive models (GAMs, Wood, 2017) of the form $x_t = s(x_{t-1}) + \varepsilon_t$ and tested time-varying linear models with dynamic linear models (DLM). GAMs allow one to model the effect of a covariate as a flexible non-linear function while DLMs allow the effect of the covariate to vary over time. Our GAM approach is analogous to that taken by Jacobson and MacCall (1995) in a study of the effects of SST on Pacific sardine recruitment.

The first step in our analysis was to determine the catch model: the model for current catch as a function of the past catch. We explored four classes of models: null models with a simple function of prior catch, linear regressive models with one to two years of prior catch, dynamic linear models (DLM) which allow the regression parameters to vary (Holmes et al., 2012, using the MARSS package in R), and GAMs to allow the effect of prior catch to be non-linear. One feature of GAMs is that they allow the smoothing parameter of the response curve to be estimated. We fixed the smoothing parameter at an intermediate value so that smooth responses were achieved. Multi-modal or overly flexible response curves would not be realistic for our application. We fit GAMs with smooth terms represented by penalized regression splines (Wood, 2011, using the mgcv package in R) and fixed the smoothing term at an intermediate value (sp=0.6).

We compared the following catch models:

- null: $ln(C_{i,t}) = ln(C_{j,t-1})$
- random walk: $ln(C_{i,t}) = \alpha + ln(C_{j,t-1})) + \varepsilon_t$
- linear AR-1: $ln(C_{i,t}) = \alpha + \beta ln(C_{j,t-1})) + \varepsilon_t$
- linear AR-2: $ln(C_{i,t}) = \alpha + \beta_1 ln(C_{j,t-1})) + \beta_2 ln(C_{k,t-2})) + \varepsilon_t$
- DLM AR-1: $ln(C_{i,t}) = \alpha_t + \beta_t ln(C_{j,t-1})) + \varepsilon_t$
- GAM AR-1: $ln(C_{i,t}) = \alpha + s(ln(C_{j,t-1})) + \varepsilon_t$
- GAM AR-2: $ln(C_{i,t}) = \alpha + s_1(ln(C_{j,t-1})) + s_2(ln(C_{k,t-2})) + \varepsilon_t$

$ln(C_{i,t})$ is the log catch in the current year t in season i. We modeled two different catches: S_t (Jul-Sep) and N_t (Oct-Jun). The catches were logged to stabilize and normalize the variance. $s()$ is a non-linear function estimated by the GAM algorithm. The model is primarily statistical, meaning it should not be thought of as a population growth model. We tested models with prior year and two years prior Oct-Mar catch (N_{t-1} and N_{t-2}) and Jul-Sep catch (S_{t-1} and S_{t-2}) as the explanatory catch variable. S_t was not used as a predictor for N_t because S_t is the quarter immediately prior to N_t and would not be available for a forecast model since time is required to process landings data. The catch models were fit to 1984 to 2015 catch data, corresponding to the years when the SST, upwelling and precipitation data were available. F-tests, AIC and leave-one-out cross-validation (LOOCV) on nested sets of models (Wood et al., 2016) were used to evaluate the support for the catch models and later for the covariate models. LOOCV involves leaving out a data point, fitting the model, and then predicting the left-out data point. The root mean squared error (RMSE) is reported for the set of prediction errors (one for each left out data point). After selection of the best model with the 1984-2015 data, the fitting was repeated with the 1956-1983 catch data to confirm the form of the catch models. An influential years test was done by removing each year and repeating the model selection analysis.

Once the catch models were determined, the covariates were studied individually and then jointly. As with the catch models, F-tests, AIC and LOOCV (leave-one-out cross-validation) on nested sets of models were used to evaluate the support for models with covariates. The smoothing term was fixed at an intermediate value (sp=0.6) instead of being treated as an estimated variable. Our models for catch with covariates took the form $ln(C_{i,t}) = M + \alpha + s_1(V_{1,t}) + s_2(V_{2,t-1}) + \varepsilon_t$, $ln(C_{i,t}) = M + \alpha + \beta_1 V_{1,t} + \beta_2 V_{2,t-1} + \varepsilon_t$, and $ln(C_{i,t}) = M + \alpha + \beta_t V_{1,t} + \varepsilon_t$ where M was the best catch model from step 1 and V is a covariate. Thus models with covariates modeled as a linear, non-linear and time-varying effect were compared. The covariates tested are those hypothesized to drive variability in oil sardine landings (Table 1). We tested both models with one and two covariates and did not use correlated covariates in the same model.

Results

Catches in prior seasons as explanatory variables

Using the 1984-2015 catch data, the time-period that overlaps our available environmental data, the Jul-Sep catch models were compared against a "naive" model in which the forecasted Jul-Sep catch is the Jul-Sep catch in the prior year. The "naive" model has no estimated parameters and is a standard null model for time series modeling. Models with $ln(N_{t-1})$ (Oct-Mar catch in prior year) as the explanatory covariate were strongly supported over the naive model and over models with $ln(S_{t-1})$ (Jul-Sep catch in prior year) as the explanatory variable (Tables A1 and A2). Addition of the catch two years prior, $ln(N_{t-2})$ or $ln(S_{t-2})$, was not supported (by AIC or F-tests) for either the linear or non-linear models. We tested the support for non-linearity in the effect of the prior year catch by comparing models with $ln(N_{t-1})$ or $ln(S_{t-1})$ included as a linear effect or as a non-linear effect using GAMs (Table A2). The residual error decreased using a non-linear response and LOOCV decreased but at the cost increased degrees of freedom. Overall there were three models with almost idential AIC and LOOCV: linear and non-linear with $ln(N_{t-1})$, and non-linear with $ln(N_{t-1})$ and $ln(N_{t-2})$. We choose the non-linear with $ln(N_{t-1})$ as the base catch model based on further diagnostic tests (described below) and to minimize loss of degrees of freedom. The adjusted R^2 of this model was 24.4%.

The model selection results were similar for models of the Oct-Mar landings (N_t), but the models explained much more of the variance (with a maximum adjusted $R^2 = 56.6$). The most supported model for N_t (Tables A3 and A4) based on AIC and F-tests used a non-linear response to Oct-Mar catch of the previous season $ln(N_{t-1})$ plus a non-linear response to Jul-Sep catch two years prior $ln(S_{t-2})$, however the LOOCV (out of sample prediction accuracy) was higher than the naive null model. The simpler model with only $ln(N_{t-1})$ had the second lowest AIC and the lowest LOOCV (and lower than the naive null model). This simpler model was also included as one of the base models for the Oct-Mar catch.

As diagnostic checks, we repeated the model comparisons with the landings data set from 1956 to 1983. The results were the same for the Jul-Sep catch (Table A5) with the model with $ln(N_{t-1})$ included as a non-linear covariate giving the lowest AIC and LOOCV. For the Oct-Mar catch (Table A6), the results were very similar but not identical. The model with $ln(N_{t-1})$ included as a non-linear covariate had the lowest LOOCV while the models with $ln(N_{t-1})$ and $ln(S_{t-2})$ or $ln(S_{t-2})$ had the lowest AIC (though less than 1 from the AIC of the $ln(N_{t-1})$ model). We also did an influential years test using leave-one-out cross-validation (Appendix F). This test involved leaving out one year and repeating the model selection tests. This analysis supported the selected base models using the 1984-2015 data. The dynamic linear models (allowing a time-varying effect of prior catch) performed poorly for the Jul-Set catch with high AIC and LOOCV. For the Oct-Mar catch, the performance was mixed with higher AIC but lower LOOCV for one of the DLMs.

Based on the model selection tests, the following non-linear model was chosen as the base model for Jul-Sep (S_t) catch:

$$M0 : ln(S_t) = \alpha + s(ln(N_{t-1})) + \varepsilon_t.$$

Two base non-linear models were chosen for Oct-Mar (N_t) catch:

$$M1 : ln(N_t) = \alpha + s_1(ln(N_{t-1})) + s_2(ln(S_{t-2})) + \varepsilon_t$$

$$M2 : ln(N_t) = \alpha + s(ln(N_{t-1})) + \varepsilon_t$$

Note that although M0 was the best model for Jul-Sep catch, it was only weakly explanatory. The maximum adjusted R^2 was less than 30% (Table A2). For the Oct-Mar catch, M1 and M2 were more explanatory with an adjusted R^2 of 45.3% for M1 and 56.6% for M2 (Table A4).

Environmental covariates as explanatory variables

There was no support for using precipitation during the summer monsoon (June-July) or pre-monsoon period (April-May) as an explanatory variable for the Jul-Sep or Oct-Mar catch (hypotheses S1 and S2; Tables B1, B2 and B3). This was the case whether precipitation in the current or previous season was used, if precipitation was included as a non-linear or non-linear effect, and if either precipitation during monsoon (June-July) or pre-monsoon (April-May) was used as the covariate. Jul-Sep overlaps with the late spawning period and precipitation is often thought to trigger spawning, however we were unable to find any consistent association of catch with precipitation. Raja (1974) posited that the appropriate time period for the effect of rainfall is the weeks before and after the new moon when spawning is postulated to occur and not the total rainfall during the monsoon season. Thus the lack of correlation may be due to using too coarse of a time average for the precipitation.

The sea-surface temperature before spawning (March-May) has been speculated to be correlated with successful egg development and spawning behavior (hypothesis S4 and S5) and extreme heat events in the pre-spawning period have been associated with low recruitment. This suggests that March-May in the current and prior years should be associated with low catch. The sea-surface temperature during larval and early juvenile development (October-December) may affect survival and growth in multiple ways and thus would correlated with biomass in future years (hypothesis L1). However we found no support for either of these SST covariates as explanatory variables for the Jul-Sep catch and only weak support (based on AIC) for March-May SST in the current season for explaining variability in Oct-Mar catch. The fall average SST in the prior season did not explain variability in either Jul-Sep or Oct-Mar catch. See Tables B4, B5 and B6. We also found no correlation between the ONI index (hypothesis A2) for either the Jul-Sep or Oct-Mar catch (Tables B7, B8 and B9).

Instead we found support for the covariates indirectly and directly associated with productivity and food availability: upwelling intensity and surface chlorophyll. The correlation between landings and upwelling was only found for upwelling in the current season. No correlation was found when we used the upwelling index from the prior season. The correlation between landings and upwelling was found for both Jul-Sep and Oct-Mar landings and with either SST-based upwelling index: average nearshore SST along the Kerala coast during June-September or the average SST nearshore versus offshore differential (UPW) off Kochi in June-September (Table 2, B4, B5 and B6). These two upwelling indices are correlated but not identical. The model with average June-September nearshore SST was more supported than the model using the SST differential off Kochi. For Jul-Sep catch, this model with a non-linear response had an adjusted R^2 of 41.0 versus an adjusted R^2 of 24.4 for the model with no covariates (Table B4), and for Oct-Mar catch, the adjusted R^2 was 61.8 versus 56.6 (Table B5). Note, that this covariate is June-September in the current season and overlaps with the July-September catch. Thus this model cannot be used to forecast Jul-Sep catch and gives only a month-prior forecast for Oct-Mar, but it does help us understand what factors may be influencing catch.

Chlorophyll-a density is speculated to be an important predictor of larval sardine survival and growth. In addition, sardines shoal in response to coastal chlorophyll blooms, which brings them in contact with the coastal fisheries. Thus chlorophyll-a density is assumed to be an important driver of future or current sardine catches. We only have chlorophyll-a remote sensing data from 1998 onward. Our simplest covariate model required 5 degrees of freedom, thus we were limited in the analyses we could conduct. In addition, the years, 1998-2014, have relatively low variability in catch sizes; the logged catch sizes during this period range from 10-11 during Jul-Sep and 11-12 during the other three quarters. Second degree polynomial models were fit (Appendix C) to the average log chlorophyll-a density in the current and prior season from quarter 3 (July-September), 4 (October-December), and 1 (January-March). Chlorophyll-a density was not a significant predictor for the Jul-Sep catch for any of the tested combinations of current or prior season and quarter. The only significant effect was seen for Oct-Mar monsoon catches using chlorophyll-a density in Oct-Dec of the prior season (Table C1). This is in contrast to the results with monsoon upwelling indices, which found a correlation with the current season but not prior seasons.

The strongest correlation however was found with the multi-year average sea surface temperature for the nearshore waters off Kerala, latitude 8 to 11 (Table 2, B7, B8 and B9). The average sea surface temperature over multiple prior years has been found to be correlated with sardine recruitment in Pacific sardines (Checkley et al., 2017; Jacobson & MacCall, 1995; Lindegren et al., 2013) and southern African sardines (Boyer et al., 2001). We tested as a model covariate the average SST for 2.5 years prior to the Jul-Sep catch, so January-June in the current calendar year and the two prior calendar years for a 30-month average. This covariate can be used for forecasting since it does not overlap with either Jul-Sep or Oct-Mar catch. This covariate with a non-linear response was the best covariate for both the Jul-Sep and Oct-Mar catch. For Oct-Mar catch, the model with multi-year average SST had an adjusted R^2 of 67.5 versus 56.6 without. For the Jul-Sep catch, the adjusted R^2 was 41.0 versus 24.4 without the multi-year average SST covariate. The response curve was step-like with a negative effect at low temperatures and then an positive flat effect at higher temperatures (Figure 5). This is similar to the step-response found in studies of the correlation between average SST and recruitment in Pacific sardines (Jacobson & MacCall, 1995).

The only other strong correlation was found for Oct-Mar catch with the DMI in the prior season. The Dipole Mode Index in the prior year has been shown to be correlated with nearshore anoxia off the Kerala coast (Vallivattathillam et al., 2017). However this correlation was only found with the Oct-Mar catch using the base model with both N_{t-1} and S_{t-2}. The correlations with the multi-year SST average was more robust and found with both Oct-Mar base models and also for Jul-Sep catch.

Discussion

Sardines in all the world's ecosystems exhibit large fluctuations in abundance (Baumgartner et al., 1992). These small forage fish are strongly influenced by natural variability in the ocean environment. Upwelling, influenced by both large-scale forces such as regimes shifts and El Niño/Southern Oscillation patterns (Alheit & Hagen, 1997; Schwartzlose et al., 2010) and by seasonal wind and current patterns, brings nutrient rich and oxygen rich waters to the surface. This drives the seasonal variability in phytoplankton resources and in turn sardine prey (Bakun et al., 2008). Local variability in temperature, salinity, and oxygen levels have both direct and indirect on sardine reproduction, recruitment and survival (Checkley et al., 2017). Sardines are also influenced by competition and predation by other species and well-known for their sensitivity to over-fishing which has been linked to many fishery collapses (Kripa et al., 2018).

Many studies on Pacific sardines have looked at the correlation between ocean surface temperature (SST) and recruitment. Temperature can have direct effect on larval survival and growth and an indirect effect on food availability. Studies in the California Current System, have found that SST explains (a portion of) year-to-year variability in Pacific sardine recruitment (Checkley et al., 2009, 2017; Jacobson & MacCall, 1995; Lindegren & Checkley, 2012) and that the average nearshore temperature over multiple seasons is the relevant explanatory variable. Similar to these studies, we found that the average nearshore SST over multiple seasons was the covariate that explained the most variability in catch both in the monsoon and post-monsoon months. McClatchie et al. (2010) found no SST relationship with SST and Pacific sardine recruitment, however their analysis used a linear relationship while the other studies, and ours, that found a relationship allowed a non-linearity. Both Jacobson and Mac-

Call (1995) and Checkley et al. (2017) found a step-like response function for temperature: below a threshold value the effect of temperature was linear and above the threshold, the effect was flat and at lower temperatures the effect was negative and became positive as temperature increased. Our analysis found a similar pattern with a negative effect when the 2.5-year average temperature was below 28.35°C and positive above and with the positive effect leveling off above 28.5°C (Figure 5).

There were four outlier years when Kerala oil sardine landings were much lower than expected based on prior catches: 1986, 1991, 1994 and 2013. The 2.5-year average SST predicted the collapses in 1986 and 1991 (Figure 6); the size of the residual with the covariate was much smaller than without the covariate. The largest collapse was in 1994 and the most recent, in our dataset, was 2013. The 2.5-year average SST did not predict the 1994 nor 2013 collapse. There was no change in the size of the residual with and without the covariate. In fact, none of the covariates we tested changed the size of the model residuals for 1994 nor 2013. The causes of these unusual declines appear unrelated to the environmental factors we studied. This suggests either that other factors, biological or anthropogenic, drove these declines or that a particular combination of environmental factors led to the declines. It should also be noted that our upwelling indices captured only one aspect of upwelling: the nearshore intensity. Other aspects of upwelling also affect oil sardines, such as the spatial extent both along the coast and off the coast and the timing of the start of upwelling.

Seasonal productivity in the SE Arabian Sea upwelling system is driven by the summer monsoon, which causes strong coastal upwelling that moves from the south to the north over the summer. This drives a strong seasonal pattern of zooplankton abundance (Figure 3). Despite the strong connection between sardine recruitment, growth and survival with upwelling, we found no correlation upwelling in the prior season with landings. We did find a correlation between upwelling in the current season with landings in the current season. The biological reasons behind a positive relationship with upwelling are clear. Upwelling drives productivity and higher food resources in the current season leads to higher recruitment and higher numbers of 0-year fish in the landings and brings sardines into the nearshore to feed where they are exposed to the fishery. However, the explanatory power of the upwelling indices was mainly due to the negative effect of extremely high upwelling (Figure 5). Extremely high upwelling transports larval sardines offshore and can create regions of low oxygen which sardines avoid.

One of the purposes of our research was to investigate environmental covariates that would improve prediction of landings, specific reduce the errors from a basic auto-correlated model using only past catch. In Table 2, the out of sample prediction errors are shown in the LOOCV

RMSE (leave-one-out cross-validation root-mean-square error) column. The simpler catch models, with only N_{t-1} as the covariate have better predictive performance than a null model which uses only last years catch (in the same period) as the prediction. For Jul-Sep, the addition of the best covariates only improves the predictions for one covariate, Jun-Sep SST. The Jul-Sep catch is difficult to forecast. It has high variability that is poorly explained by past catch or the environment. In contrast, the Oct-Mar catch is much better explained by prior catch (higher R^2) and by the multi-year temperature. The multi-year average SST reduced the prediction errors using either the more complex base model with two years of past catch as the covariate (from LOOCV 1.062 to 0.827) and the simpler base model with only the prior year catch (from LOOCV 0.966 to 0.796).

Conclusions

Remote sensing satellites can be used to detect changes in ocean physical, biological and chemical properties, such as surface temperature, winds, surface height, surface waves, rainfall and surface salinity, as well as the ecosystem and water quality changes. Unlike in-situ measurements, environmental measures from remote-sensing can be acquired rapidly and over large regions. However, which environmental covariates will improve forecasts is not obvious from oil sardine life-history alone. We tested many of the covariates known or suspected to have an effect on sardine spawning, growth and survival (Table 1): precipitation, upwelling indices, ocean temperature and chlorophyll-a in various critical months of the sardine life-cycle. We found that the multi-year average nearshore ocean temperature explained the most variability in the landings. This covariate is not as directly tied to stages of the oil sardine life-cycle as the other covariates we tested, though it does integrate over multiple influences (upwelling strength and temperature) over multiple years.

The temperature of the Western Indian Ocean, of which the Southeast Arabian Sea is a part, has been increasing over the last century at a rate higher than any other tropical ocean (Roxy et al., 2014) and the warming has been most extreme during the summer monsoon months. This ocean climate change is affecting oil sardine distributions with significant landings now occurring north of Goa (Vivekanandan et al., 2009). Continued warming is expected to affect the productivity of the region via multiple pathways, including both the direct effects of temperature change on the physiology and behavior of organisms and a multiple of indirect effects (Moustahfid et al., 2018). These indirect effects include changes to salinity, oxygen concentrations, currents, wind patterns, ocean stratification and upwelling spatial patterns, phenology, and intensity. Incorporating environmental covariates into landings forecasts has the potential to improve fisheries management for small pelagics such as oil sardines in the face of a changing ocean environment (Haltuch et al., 2019; Tommasi et al., 2016). However, monitoring forecast performance and covariate performance in models will be crucial as a changing ocean environment may also change the association between landings and average sea surface temperature.

References

Alheit, J., & Hagen, E. (1997). Long-term climate forcing of European herring and sardine populations. *Fisheries Oceanography*, *6*, 130–139. https://doi.org/10.1046/j.1365-2419.1997.00035.x

Alheit, J., Pohlmann, T., Casini, M., Greve, W., Hinrichs, R., Mathis, M., … Wagner, C. (2012). Climate variability drives anchovies and sardines into the North and Baltic Seas. *Progress in Oceanography*, *96*, 128–139. https://doi.org/10.1016/j.pocean.2011.11.015

Annigeri, G. G. (1969). Fishery and biology of the oil sardine at Karwar. *Indian Journal of Fisheries*, *16*(1/2), 35–50.

Antony Raja, B. T. (1964). Some aspects of spawning biology of Indian oil sardine Sardinella longiceps Valenciennes. *Indian Journal of Fisheries*, *11*(1), 45–120.

Antony Raja, B. T. (1969). Indian oil sardine. *CMFRI Bulletin*, *16*, 1–142.

Antony Raja, B. T. (1970). Estimation of age and growth of the Indian oil sardine, Sardinella longiceps Val. *Indian Journal of Fisheries*, *17*(1&2), 26–42.

Antony Raja, B. T. (1974). Possible explanation for the fluctuation in abundance of the Indian oil sardine, Sardinella longiceps Valenciennes. *Proceedings of the Indo-Pacific Fisheries Council*, *15*(3), 241–252.

Bakun, A., Roy, C., & Lluch-Cota, S. (2008). Coastal upwelling and other processes regulating ecosystem productivity and fish production in the western Indian Ocean. In K. Sherman, E. N. Okemwa, & M. J. Ntiba (Eds.), *Large marine ecosystems of the Indian ocean : Assessment, sustainability and management* (pp. 103–141). Londres: Blackwell.

Baumgartner, T. R., Soutar, A., & Ferreira-Bartrina, V. (1992). Reconstruction of the history of the Pacific sardine and northern anchovy populations over the past two millennia from sediments of the Santa Barbara basin, California. *CalCOFI Report*, *33*, 24–40.

Bensam, P. (1964). Growth variations in the Indian oil sardine, Sardinella longiceps Valenciennes. *Indian Journal of Fisheries*, *11 A*(2), 699–708.

Boyer, D. C., Boyer, H. J., Fossen, I., & Kreiner, A. (2001). Changes in abundance of the northern Benguela sardine stock during the decade 1990 to 2000 with comments on the relative importance of fishing and the environment. *South African Journal of Marine Science*, *23*, 67–84. https://doi.org/10.2989/025776101784528854

BR, S. (2010). *Coastal upwelling of the south eastern Arabian Sea — an integrated approach*. Kerala, India: PhD Thesis. Physical Oceanography. Cochin University of Science; Technology.

BR, S., Sanjeevan, V. N., Vimalkumar, K. G., & Revichandran, C. (2008). On the upwelling of the southern tip and along the west coast of India. *Journal of Coastal Research*, *24*(4C), 95–102. https://doi.org/10.2112/06-0779.1

Chauhan, O. S., Raghavan, B. R., Singh, K., Rajawat, A. S., Kader, U., & Nayak, S. (2011). Influence of orographically enhanced SW monsoon flux on coastal processes along the SE Arabian Sea. *Journal of Geophysical Research. Oceans*, *116*(12), C12037. https://doi.org/10.1029/2011JC007454

Checkley, D. M., Alheit, J., Oozeki, Y., & Roy, C. (2009). *Climate change and small pelagic fish*. https://doi.org/10.1017/CBO9780511596681

Checkley, D. M., Asch, R. G., & Rykaczewski, R. R. (2017). Climate, anchovy, and sardine. *Annual Review of Marine Science*, *9*, 469–493. https://doi.org/10.1146/annurev-marine-122414-033819

Chidambaram, K. (1950). Studies on the length frequency of oil sardine, Sardinella longiceps Cuv. & Val. And on certain factors influencing their appearance on the Calicut coast of the Madras Presidency. *Proceedings of Indian Academy of Sciences*, *31*, 352–286.

Cohen, Y., & Stone, N. (1987). Multivariate time series analysis of the Canadian fisheries system in Lake Superior. *Canadian Journal of Fisheries and Aquatic Sciences*, *44*, 171–181. https://doi.org/10.1139/f87-321

Cury, P., Bakun, A., Crawford, R. J. M., Jarre, A., Quinones, R. A., Shannon, L. J., & Verheye, H. M. (2000). Small pelagics in upwelling systems: Patterns of interaction and structural changes in "wasp-waist" ecosystems. *ICES Journal of Marine Science*, *57*(3), 603–

618. https://doi.org/10.1006/jmsc.2000.0712

Das, P. H. D., & Edwin, L. (2018). Temporal changes in the ring seine fishery of Kerala, India. *Indian Journal of Fisheries*, *65*(1), 47–54. https://doi.org/10.21077/ijf.2018.65.1.69105-08

Farmer, N. A., & Froeschke, J. T. (2015). Forecasting for recreational fisheries management: What's the catch? *North American Journal of Fisheries Management*, *35*, 720–735. https://doi.org/10.1080/02755947.2015.1044628

Garza-Gil, M. D., Varela-Lafuente, M., Caballero-Míguez, G., & Torralba-Cano, J. (2015). A study on economic impact on the European sardine fishery due to continued global warming. In B. R. Singh (Ed.), *Global warming: Causes, impacts and remedies* (pp. 115–136). https://www.doi.org/10.5772/58877

Georgakarakos, S., Doutsoubas, D., & Valavanis, V. (2006). Time series analysis and forecasting techniques applied on loliginid and ommastrephid landings in Greek waters. *Fisheries Research*, *78*, 55–71. https://doi.org/10.1016/j.fishres.2005.12.003

George, G., Meenakumari, B., Raman, M., Kumar, S., Vethamony, P., Babu, M. T., & Verlecar, X. (2012). Remotely sensed chlorophyll: A putative trophic link for explaining variability in Indian oil sardine stocks. *Journal of Coastal Research*, *28*(1A), 105–113. https://doi.org/10.2112/JCOASTRES-D-10-00070.1

Habeebrehman, H., Prabhakaran, M. P., Jacob, J., Sabu, P., Jayalakshmi, K. J., Achuthankutty, C. T., & Revichandran, C. (2008). Variability in biological responses influenced by upwelling events in the eastern Arabian Sea. *Journal of Marine Systems*, *74*, 545–560. https://doi.org/10.1016/j.jmarsys.2008.04.002

Haltuch, M. A., Brooks, E. N., Brodziak, J., Devine, J. A., Johnson, K. F., Klibansky, N., … Wells, B. K. (2019). Unraveling the recruitment problem: A review of environmentally-informed forecasting and management strategy evaluation. *Fisheries Research*, *217*, 198–216. https://doi.org/10.1016/j.fishres.2018.12.016

Hanson, P. J., Vaughan, D. S., & Narayan, S. (2006). Forecasting annual harvests of Atlantic and Gulf menhaden. *North American Journal of Fisheries Management*, *26.3*, 753–764. https://doi.org/10.1577/M04-096.1

Holmes, E. E., Ward, E. J., & Wills, K. (2012). MARSS: Multivariate autoregressive state-space models for analyzing time-series data. *R Journal*, *4*, 11–19.

Hornell, J. (1910). Report on the results of a fishery cruise along the Malabar coast and to the Laccadive Islands in 1908. *Madras Fishery Bulletin*, *4*(4), 76–126.

Hornell, J., & Nayudu, M. R. (1923). A contribution to the life history of the Indian sardine with note, on the plankton of the Malabar coast. *Madras Fishery Bulletin*, *17*, 129.

Jacobson, L. D., & MacCall, A. D. (1995). Stock-recruitment models for Pacific sardine (Sardinops sagax). *Canadian Journal of Fisheries and Aquatic Sciences*, *52*, 566–577. https://doi.org/10.1139/f95-057

Jayaprakash, A. A. (2002). Long term trends in rainfall, sea level and solar periodicity: A case study for forecast of Malabar sole and oil sardine fishery. *Journal of the Marine Biological Association of India*, *44*(1 & 2), 163–175.

Jayaprakash, A. A., & Pillai, N. G. K. (2000). The Indian oil sardine. In V. N. Pillai & N. G. Menon (Eds.), *Marine fisheries research and management* (pp. 259–281). Kerala, India: Central Marine Fisheries Research Institute.

Jayaram, C., Chacko, N., Joseph, K. A., & Balchand, A. N. (2010). Interannual variability of upwelling indices in the southeastern Arabian Sea: A satellite based study. *Ocean Science Journal*, *45*(1), 27–40. https://doi.org/10.1007/s12601-010-0003-6

Kripa, V., Mohamed, K. S., Koya, K. P. S., Jeyabaskaran, R., Prema, D., Padua, S., … Vishnu, P. G. (2018). Overfishing and climate drives changes in biology and recruitment of the Indian oil sardine Sardinella longiceps in southeastern Arabian sea. *Frontiers in Marine Science*, *5*, Article 443. https://doi.org/10.3389/fmars.2018.00443

Krishnakumar, P. K., Mohamed, K. S., Asokan, P. K., Sathianandan, T. V., Zacharia, P. U., Abdurahiman, K. P., … Durgekar, N. R. (2008). How environmental parameters influenced fluctuations in oil sardine and mackerel fishery during 1926-2005 along the south-west coast of India? *Marine Fisheries Information Service, Technical and Extension Series*, *198*, 1–5.

Lawer, E. A. (2016). Empirical modeling of annual fishery landings. *Natural Resources*, *7*, 193–204. https://doi.org/10.4236/nr.2016.74018

Lindegren, M., & Checkley, D. M. (2012). Temperature dependence of Pacific sardine (Sardinops sagax) recruitment in the California Current Ecosystem revisited and revised. *Canadian Journal of Fisheries and Aquatic Sciences*, *70*(2), 245–252. https://doi.org/10.1139/cjfas-2012-0211

Lindegren, M., Checkley, D. M., Rouyer, T., MacCall, A. D., & Stenseth, N. C.

(2013). Climate, fishing, and fluctuations of sardine and anchovy in the California Current. *Proceedings of the National Academy of Sciences*, *110*(33), 13672–13677. https://doi.org/10.1073/pnas.1305733110

Lloret, J., Lleonart, J., & Sole, I. (2000). Time series modelling of landings in Northwest Mediterranean Sea. *ICES Journal of Marine Science*, *57*, 171–184. https://doi.org/10.1006/jmsc.2000.0570

Longhurst, A. R., & Wooster, W. S. (1990). Abundance of oil sardine (Sardinella longiceps) and upwelling on the southwest coast of India. *Canadian Journal of Fisheries and Aquatic Sciences*, *47*(12), 2407–2419. https://doi.org/10.1139/f90-268

Madhupratap, M., Gopalakrishnan, T. C., Haridas, P., & Nair, K. K. C. (2001). Mesozooplankton biomass, composition and distribution in the Arabian Sea during the fall intermonsoon: Implications of oxygen gradients. *Deep Sea Research Part II: Topical Studies in Oceanography*, *48*(6), 1345–1368. https://doi.org/10.1016/S0967-0645(00)00142-9

Madhupratap, M., Shetye, S. R., Nair, K. N. V., & Nair, S. R. S. (1994). Oil sardine and Indian mackerel: Their fishery, problems and coastal oceanography. *Current Science*, *66*(5), 340–348. https://doi.org/10.1029/2004GL019652

McClatchie, S., Goericke, R., Auad, G., & Hill, K. (2010). Re-assessment of the stock–recruit and temperature–recruit relationships for Pacific sardine (Sardinops sagax). *Canadian Journal of Fisheries and Aquatic Sciences*, *67*(11), 1782–1790. https://doi.org/10.1139/F10-101

Mendelssohn, R. (1981). Using Box-Jenkins models to forecast fishery dynamics: Identification, estimation and checking. *Fishery Bulletin*, *78*, 887–896.

Menon, N. N., Sankar, S., Smitha, A., George, G., Shalin, S., Sathyendranath, S., & Platt, T. (2019). Satellite chlorophyll concentration as an aid to understanding the dynamics of Indian oil sardine in the southeastern Arabian Sea. *Marine Ecology Progress Series*, *617-618*, 137–147. https://doi.org/10.3354/meps12806

Moustahfid, H., Marsac, F., & Grangopadhyay, A. (2018). Climate change impacts, vulnerabilities and adaptations: Western Indian ocean marine fisheries. In M. Barange, T. Bahri, M. C. M. Beveridge, K. L. Cochrane, S. Funge-Smith, & F. Poulain (Eds.), *Impacts of climate change on fisheries and aquaculture: Synthesis of current knowledge, adaptation and mitigation options* (pp. 251–280). Rome: FAO Fisheries; Aquaculture Technical Paper No. 627.

Murty, A. V. S., & Edelman, M. S. (1966). On the relation between the intensity of the south-west monsoon and the oil-sardine fishery of India. *Indian Journal of Fisheries*, *13*(1 & 2), 142–149.

Naidu, P. D., Kumar, M. R. R., & Babu, V. R. (1999). Time and space variations of monsoonal upwelling along the west and east coasts of India. *Continental Shelf Research*, *19*(4), 559–572. https://doi.org/10.1016/S0278-4343(98)00104-6

Nair, P. G., Joseph, S., Kripa, V., Remya, R., & Pillai, V. N. (2016). Growth and maturity of Indian oil sardine Sardinella longiceps (Valenciennes, 1847) along south-west coast of India. *Journal of Marine Biological Association of India*, *58*(1), 64–68. https://doi.org/10.6024/jmbai.2016.58.1.1899-07

Nair, R. V. (1952). Studies on the revival of the Indian oil sardine fishery. *Proceedings of Indo-Pacific Fisheries Council*, *2*, 1–15.

Nair, R. V. (1959). Notes on the spawning habits and early life-history of the oil sardine, Sardinella longiceps Cuv. & Val. *Indian Journal of Fisheries*, *6*(2), 342–359.

Nair, R. V., & Subrahmanyan, R. (1955). The diatom, Fragilaria oceanica Cleve, an indicator of abundance of the Indian oil sardine, Sardinella longiceps Cuv. And Val. *Current Science*, *24*(2), 41–42.

Nobel, A., & Sathianandan, T. V. (1991). Trend analysis in all-India mackerel catches using ARIMA models. *Indian Journal of Fisheries*, *38*(2), 119–122.

Pillai, V. N. (1991). Salinity and thermal characteristics of the coastal waters off southwest coast of India and their relation to major pelagic fisheries of the region. *Journal of the Marine Biological Association of India*, *33*(1&2), 115–133.

Piontkovski, S., Al Oufi, H., & Al Jufaily, S. (2015). Seasonal and interannual changes of Indian oil sardine, Sardinella longiceps, landings in the governorate of Muscat (the Sea of Oman). *Marine Fisheries Review*, *76*, 48–58. https://doi.org/10.7755/MFR.76.3.3

Pitchaikani, J. S., & Lipton, A. P. (2012). Impact of environmental variables on pelagic fish landings: Special emphasis on Indian oil sardine off Tiruchendur coast, Gulf of Mannar. *Journal of Oceanography and Marine Sciences*, *3*(3), 56–67. https://doi.org/10.5897/JOMS12.006

Prabhu, M. S., & Dhulkhed, M. H. (1967). On the occurrence of small-sized oil sardine Sardinella longiceps Val. *Current Science*, *35*(15), 410–411.

Prabhu, M. S., & Dhulkhed, M. H. (1970). The oil sardine fishery in the Mangalore zone during the seasons 1963-64 and 1967-68. *Indian Journal of Fisheries*, *17*, 57–75.

Prista, N., Diawara, N., Costa, M. J., & Jones, C. (2011). Use of SARIMA models to assess data-poor fisheries: A case study with a sciaenid fishery off Portugal. *Fisheries Bulletin*, *109*, 170–185.

Raghavan, B. R., Deepthi, T., Ashwini, S., Shylini, S. K., Kumarswami, M., Kumar, S., & Lotliker, A. A. (2010). Spring inter monsoon algal blooms in the Eastern Arabian Sea: Shallow marine encounter off Karwar and Kumbla coast using a hyperspectral radiometer. *International Journal of Earth Sciences and Engineering*, *3*(6), 827–832.

Rohit, P., Sivadas, M., Abdussamad, E. M., Rethinam, A. M. M., Koya, K. P. S., Ganga, U., … Supraba, V. (2018). *Enigmatic Indian oil sardine: An insight*. CMFRI Special Publication No. 130. p156. ICAR-Central Marine Fisheries Research Institute.

Roxy, M. K., Ritika, K., Terray, P., & Masson, S. (2014). The curious case of Indian Ocean warming. *Journal of Climate*, *27*(22), 8501–8509. https://doi.org/10.1175/JCLI-D-14-00471.1

Rykaczewski, R. R., & Checkley, D. M. (2008). Influence of ocean winds of the pelagic ecosystem in upwelling regions. *Proceedings of the National Academy of Science*, *105*(6), 1965–1970. https://doi.org/10.1073/pnas.0711777105

Schaaf, W. E., Sykes, J. E., & Chapoton, R. B. (1975). Forecasts of Atlantic and Gulf menhaden catches based on the historical relation of catch and fishing effort. *Marine Fisheries Review*, *37*, 5–9.

Schwartzlose, R. A., Alheit, J., Bakun, A., Baumgartner, T. R., Cloete, R., Crawford, R. J. M., … Zuzunaga, J. Z. (2010). Worldwide large-scale fluctuations of sardine and anchovy populations. *South African Journal of Marine Science*, *21*(1), 289–347. https://doi.org/10.2989/025776199784125962

Srinath, M. (1998). Exploratory analysis on the predictability of oil sardine landings in Kerala. *Indian Journal of Fisheries*, *45*(4), 363–374.

Srinath, M., Kuriakose, S., & Mini, K. G. (2005). Methodology for estimation of marine fish landings in India. In *CMFRI Special Publications No. 86. P57.* Central Marine Fisheries Research Institute.

Stergiou, K. I., & Christou, E. D. (1996). Modeling and forecasting annual fisheries catches: Comparison of regression, univariate and mulivariate time series methods. *Fisheries*

Research, *25*(2), 105–138. https://doi.org/10.1016/0165-7836(95)00389-4

Supraba, V., Dineshbabu, A. P., Thomas, S., Rohit, P., Rajesh, K. M., & Zacharia, P. U. (2016). Climate influence on oil sardine and Indian mackerel in southeastern Arabian sea. *International Journal of Development Research*, *6*(8), 9152–9159.

Takasuka, A., Oozeki, Y., & Aoki, I. (2007). Optimal growth temperature hypothesis: Why do anchovy flourish and sardine collapse or vice versa under the same ocean regime? *Canadian Journal of Fisheries and Aquatic Sciences*, *64*, 768–776. https://doi.org/10.1139/f07-052

Thara, K. J. (2011). *Response of eastern Arabian Sea to extreme climatic events with special reference to selected pelagic fishes*. Kerala, India: PhD Thesis. Department of Physical Oceanography. Cochin University of Science; Technology.

Tommasi, D., Stock, C. A., Pegion, K., Vecchi, G. A., Methot, R. D., Alexander, M. A., & Checkley, D. M. (2016). Improved management of small pelagic fisheries through seasonal climate prediction. *Ecological Applications*, *27*(2), 378–388. https://doi.org/10.1002/eap.1458

Vallivattathillam, P., Iyyappan, S., Lengaigne, M., Ethé, C., Vialard, J., Levy, M., … Naqvi, W. (2017). Positive Indian Ocean Dipole events prevent anoxia off the west coast of India. *Biogeosciences*, *14*(6), 1541–1559. https://doi.org/10.5194/bg-14-1541-2017

Venugopalan, R., & Srinath, M. (1998). Modelling and forecasting fish catches: Comparison of regression, univariate and multivariate time series methods. *Indian Journal of Fisheries*, *45*(3), 227–237.

Vivekanandan, E., Rajagopalan, M., & Pillai, N. G. K. (2009). Recent trends in sea surface temperature and its impact on oil sardine. In *Global climate change and Indian agriculture* (pp. 89–92).

Vivekanandan, E., Srinath, M., Pillai, V. N., Immanuel, S., & Kurup, K. N. (2003). Marine fisheries along the southwest coast of India. In G. Silvestre, L. Garces, I. Stobutzki, C. Luna, M. Ahmad, R. A. Valmonte-Santos, … D. Pauly (Eds.), *Assessment, management, and future directions for coastal fisheries in Asian countries* (pp. 759–792). WorldFish Center, Penang.: WorldFish Center Conference Proceedings 67.

Wood, S. N. (2011). Fast stable restricted maximum likelihood and marginal likelihood estimation of semiparametric generalized linear models. *Journal of the Royal Statistical Society B*, *73*(1), 3–36. https://doi.org/10.1111/j.1467-9868.2010.00749.x

Wood, S. N. (2017). *Generalized additive models: An introduction with R*. Chapman; Hall/CRC.

Wood, S. N., Pya, N., & Safken, B. (2016). Smoothing parameter and model selection for general smooth models (with discussion). *Journal of the American Statistical Association*, *111*, 1548–1575. https://doi.org/10.1080/01621459.2016.1180986

Xu, C., & Boyce, M. S. (2009). Oil sardine (Sardinella longiceps) off the Malabar coast: Density dependence and environmental effects. *Fisheries Oceanography*, *18*(5), 359–370. https://doi.org/10.1111/j.1365-2419.2009.00518.x

Figure Legends

Figure 1. Close up of Kerala State with the latitude/longitude boxes used for the satellite data. Kerala State is marked in grey and the oil sardine catch from this region is being modeled.

Figure 2. Quarterly catch data 1956-2014 from Kerala. The catches have a strong seasonal pattern with the highest catches in quarter 4 Note that quarter 3 is July-September and that the fishery is closed July 1 to August 15, thus the fishery is only open 1.5 months in quarter 3. The mean catch (metric tonnes) in quarters 1 to 4 are 38, 19.2, 30.9, and 59.9 metric tonnes respectively.

Figure 3. Key oil sardine life-history events overlaid on the monthly sea surface temperature in the nearshore and offshore and the nearshore chlorophyll density.

Figure 4. Remote sensing covariates used in the analysis. All data are monthly averages over Box 4 in Figure 1 on the Kerala coast off of Kochi. Panel A) Upwelling Index. The upwelling index is the difference between the near-shore sea surface temperature (SST) and the off-shore SST defined as 3 degrees longitude offshore. Panel B) Surface chlorophyll-a (CHL). The CHL data are only available from 1997 onward. Panel C) Sea surface temperature constructed from Advanced Very High Resolution Radiometer (AVHRR). Panel D) Average daily rainfall (mm/day) off the Kerala coast.

Figure 5. Effects of covariates estimated from the GAM models. Panel A) Effect of the 2.5 year average nearshore SST on catch during the catch during July-September (late spawning and early post-spawning) months. Panel B) Effect of upwelling (inshore/off-shore SST differential) during June-September in the current season on July-September catch. The index is the difference between offshore and inshore SST, thus a negative value indicates warmer coastal surface water than off-shore. Panel C) Effect of the 2.5 year average nearshore SST on catch during the catch during October-March (post-monsoon, age-0, -1, -2 year fish). Panel D) Effect of upwelling (inshore/off-shore SST differential) during June-September in the current season on October-March catch. Strong upwelling (positive upwelling index) in the larval and juvenile high growth period (Oct-Dec) is associated with higher early survival and larger cohorts of age-0 fish in the catch.

Figure 6. Fitted versus observed catch with models with and without environmental covariates. Panel A) Fitted versus observed log catch in the spawning months with only non-spawning catch in the previous season as the covariate: $S_t = s(N_{t-1}) + \varepsilon_t$. Panel B) Fitted versus observed log catch in July-September with the 2.5-year average nearshore SST added

as a covariate to the model in panel A. This model was: $S_t = s(N_{t-1}) + s(V_t) + \varepsilon_t$. Panel C) Fitted versus observed log catch in the post-monsoon months with only post-monsoon catch in the previous season and July-September catch two seasons prior as the covariates: $N_t = s(N_{t-1}) + s(S_{t-2}) + \varepsilon_t$. Panel D) Fitted versus observed log catch in the post-monsoon months with 2.5-year average nearshore SST (V) added as covariates. This model was $N_t = s(N_{t-1}) + s(S_{t-2}) + s(V_t) + \varepsilon_t$.

Table 1. Hypotheses for covariates affecting landings. S_t is Jul-Sep catch in the current season, S_{t-1} is Jul-Sep catch in the previous season. N_t is the Oct-Mar catch in the current season and N_{t-1} is the Oct-Mar catch in the prior season. DD = hypotheses related to effects of past abundance (landings) on current abundance. S = hypotheses related to catch during the spawning months. L = hypotheses related to larval and juvenile growth and survival. A = hypotheses affecting all ages. See the introduction for discussion of the literature on the effects of environmental covariates on sardine landings. ns-SST = nearshore SST. r-SST = regional (nearshore and offshore) SST t, $t-1$, and $t-2$ indicate current, prior, and two seasons prior.

Hypothesis	Description
DD1 $S_t \sim N_{t-1}$	S_t is age 1+ age fish and reflects the 0-2yr fish in N_{t-1} which have aged 3-6 months (Nair et al. 2016).
DD2 $S_t \sim S_{t-1} + S_{t-2}\ N_t\ S_{t-1} + S_{t-2}$	S_t is age 1+ fish and is dominated by spent post-spawning fish (Nair et al. 2016). S_t should be correlated with the abundance of the spawning stock and cohort strength. If cohort strength persists over time, landings in the current season should correlate with Jul-Sep landings in the previous two seasons.
DD3 $N_t \sim N_{t-1}$	N_{t-1} includes age 0, 1, 2 and 2+ fish (Nair et al. 2016). Thus the 0, 1, and 2 yr fish will appear 1 year later in the N_t landings.
S1 $S_t \sim$ Jun-Jul precipitation in t	The magnitude of precipitation in June-July directly or indirectly signals mature fish to spawn offshore, after which the spent adults migrate inshore to the fishery (Anthony Raja 1969, 1974; Srinath 1998).
S2 $S_t \sim$ Apr-Mar precipitation in t	If there is pre-monsoon rain during Apr-May then spawning begins earlier and spent adults return to the fishery sooner and are exposed to the fishery longer.
S3 $N_t \sim$ Apr-Mar precipitation in t	Precipitation is an indicator of climatic conditions during the period of egg development. This affect the success of spawning, thus affecting the 0-year class and the Oct-Mar catch (Antony Raja 1969, 1974; Srinath 1998).
S4 $S_t \sim$ Jun-Sep UPW in t	High rates of upwelling drive mature fish further offshore and thus leads to lower exposure to the fishery. This movement may be driven by advection of high phytoplankton biomass further offshore or increased inputs of low oxygenated water to the surface (Murty and Edelman 1970, Antony Raja 1973, Pillai et al. 1991).
S5 $S_t \sim$ Mar-May r-SST in t $N_t \sim$ Mar-May r-SST in t	Extreme heating events prior to the spring monsoon drives mature fish from the spawning areas, resulting in poor recruitment and fewer age 0 year fish in the Oct-Mar catch (Antony Raja 1973, Pillai et al 1991).

Table 1. Continued.

Hypothesis	Description
L1 $S_t \sim$ Oct-Dec ns-SST $t-1$ $N_t \sim$ Oct-Dec ns-SST $t-1$	Larval and juvenile growth and survival is affected by temperature. The temperature in the critical post-monsoon window, when somatic growth of the 0-year fish is highest, should be correlated with future abundance.
L2 $S_t \sim$ Jun-Sep UPW in $t-1$ & t $N_t \sim$ Jun-Sep UPW in $t-1$ & t	Higher upwelling rates leads to greater phytoplankton productivity, better larval and juvenile growth, and higher landings in the post monsoon Oct-March catch. However, extreme upwelling may decrease this catch, and future catches, due to poor oxygen conditions or advection of phytoplankton biomass.
L3 $S_t \sim$ CHL in $t-1$ & t $N_t \sim$ CHL in $t-1$ & t	Surface Chl-a is a proxy for phytoplankton abundance and thus food availability, so higher bloom intensities may support greater fish abundance in the current and future years.
A1 $S_t \sim$ 2.5-yr ave. ns-SST $N_t \sim$ 2.5-yr ave. ns-SST	Spawning, early survival, and recruitment of sardines depends on a multitude of cascading factors summarized by the multi-year average nearshore SST. The multi-year average SST has been correlated with recruitment and abundance in other sardines (Checkley et al. 2017) and is related to the optimal temperature windows for sardines (Takasuka et al. 2007).
A2 $S_t \sim$ ONI in $t-1$ $N_t \sim$ ONI in $t-1$	The El Nino/Southern Oscillation (ENSO) impacts a range of environmental parameters (e.g., precipitation, SST, frontal zones, winds, etc.) that may impact spawning and early survival of sardines (Supraba et al. 2016, Rohit et al. 2018).
A3 $S_t \sim$ DMI in $t-1$ $N_t \sim$ DMI in $t-1$ & t	Negative Dipole Mode Index (DMI) values in Sep-Nov are associated with anoxic events on the Kerala coast while positive values are associated with a absence of such events (Vallivattathillam et al. 2017).

Table 2. Top covariates for the monsoon (Jul-Sep) and post-monsoon (Oct-Mar) catch (S_t and N_t) models. M0, M1 and M2 are the base models with only prior catch as covariates. To the base models, the listed environmental covariates are added. The full set of covariate models and the results of the tests on the nested models sets are given in Appendix B. The LOOCV RMSE (root mean square error) is the out-of-sample prediction error. The LOOCV RSME for the null model for Jul-Sep catch was 1.599 and the LOOCV RMSE for the null model for Oct-Mar catch was 1.015. The fitted versus observed catches from the covariate models are shown in Figure 6.

Model	Residual df	Adj. R2	RMSE	AIC	LOOCV RMSE
Jul-Sep catch models with covariates					
V_t = Jun-Sep SST current season					
W_t = Jun-Sep Bakun-UPW current season					
Z_t = 2.5-year average SST					
M0: $ln(S_t) = \alpha + s(ln(N_{t-1})) + \varepsilon_t$	28.6	24	1.184	109.52	1.299
$ln(S_t) = M0 + s(V_t)$	25.9	41	1.007	103.43	1.192
$ln(S_t) = M0 + \beta W_t$	27.6	28	1.133	108.66	1.404
$\Rightarrow ln(S_t) = M1 + s(Z_t)$	26.2	41	1.011	103.26	1.338
Oct-Mar catch models with covariates					
V_t = Mar-May SST current season					
W_t = Jun-Sep SST current season					
Z_t = 2.5-year average SST					
X_t = fall DMI prior season					
M1: $ln(N_t) = \alpha + s(ln(N_{t-1})) + s(ln(S_{t-2})) + \varepsilon_t$	24.8	57	0.713	79.53	1.062
$ln(N_t) = M1 + s(V_t)$	22	63	0.628	76.01	1.002
$ln(N_t) = M1 + \beta W_t$	23.8	63	0.648	75.57	1.042
$\Rightarrow ln(N_t) = M1 + s(Z_t)$	22.7	67	0.597	71.88	0.827
$ln(N_t) = M1 + s(X_t)$	21.1	68	0.58	72.69	0.89
M2: $ln(N_t) = \alpha + s(ln(N_{t-1})) + \varepsilon_t$	27.6	45	0.836	84.75	0.966
$ln(N_t) = M2 + s(V_t)$	24.8	47	0.791	85.9	0.981
$ln(N_t) = M2 + \beta W_t$	26.6	52	0.772	81.79	0.927
$\Rightarrow ln(N_t) = M2 + s(Z_t)$	25.3	60	0.688	76.34	0.796
$ln(N_t) = M2 + s(X_t)$	23.7	43	0.8	88.43	0.969

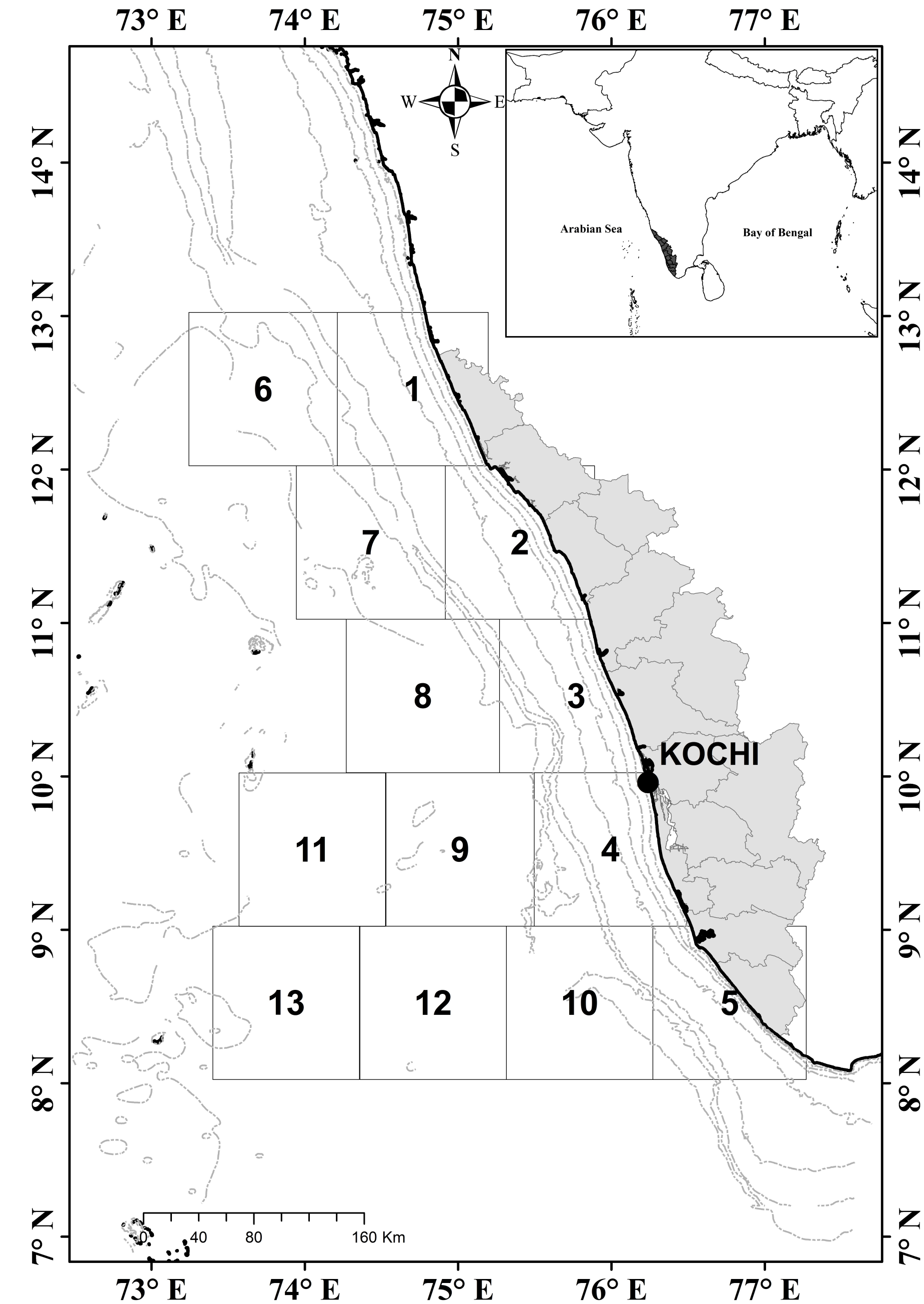
73° E
74° E
75° E
76° E
77° E
14° N
13° N
12° N
11° N
10° N
9° N
8° N
7° N
N
S
W
E
Arabian Sea
Bay of Bengal
6
1
7
2
8
3
KOCHI
11
9
4
13
12
10
5
0
40
80
160 Km

Figure 1

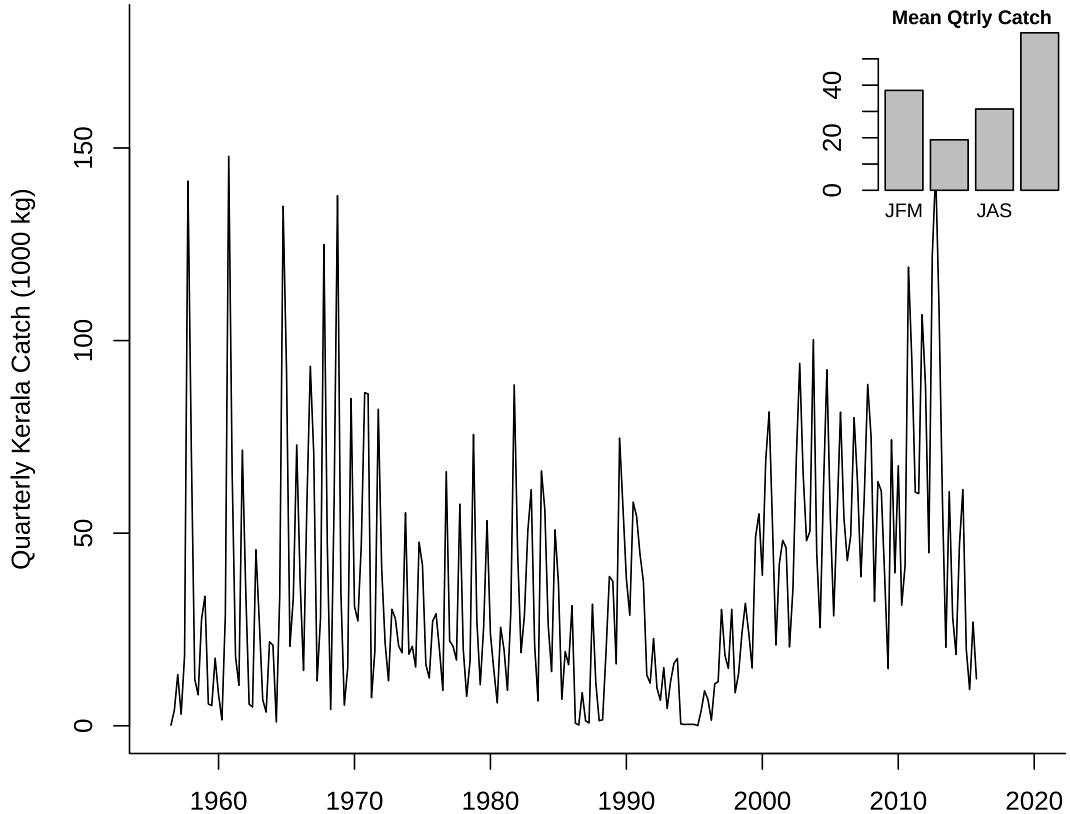
Mean Qtrly Catch
0
20
40
JFM
JAS
Quarterly Kerala Catch (1000 kg)
0
50
100
150
1960
1970
1980
1990
2000
2010
2020

Figure 2

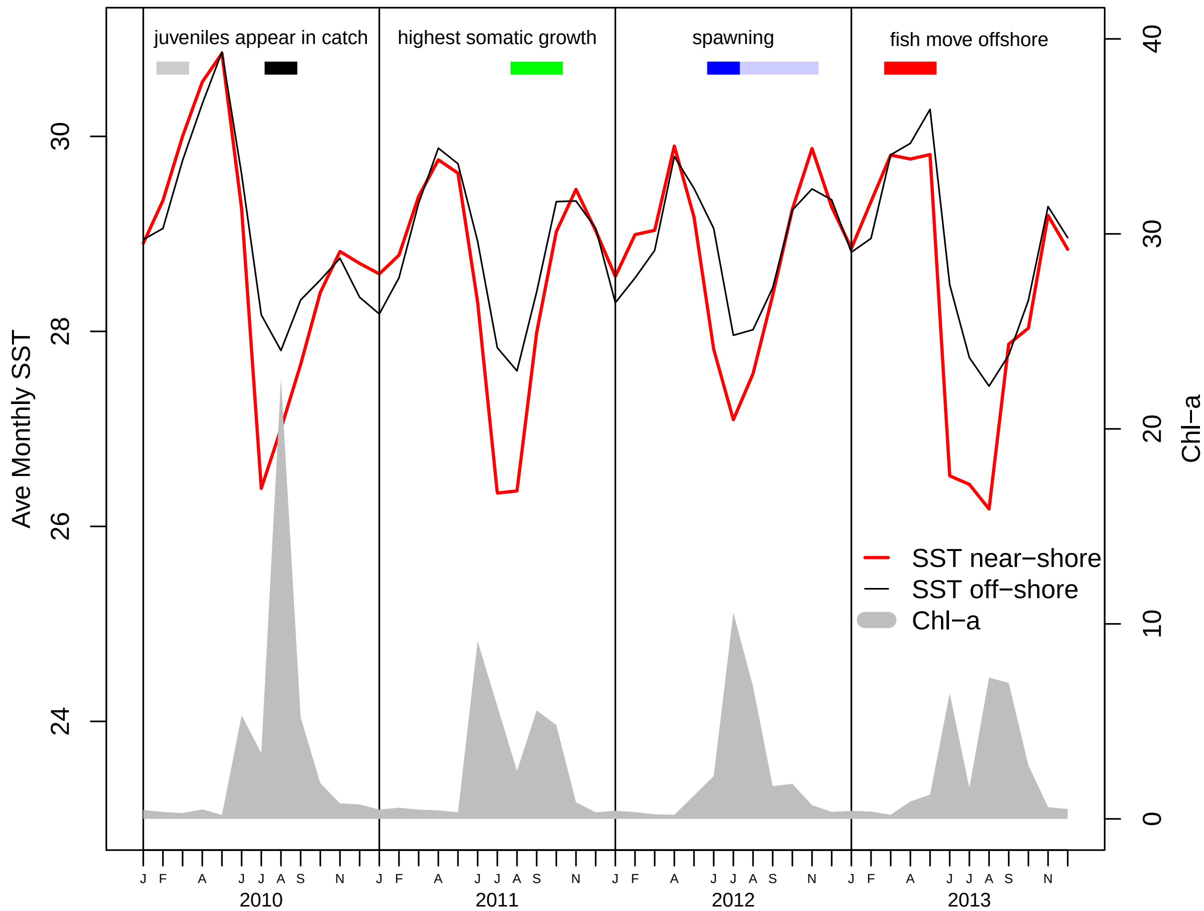

juveniles appear in catch
highest somatic growth
spawning
fish move offshore
SST near−shore
SST off−shore
Chl−a
Ave Monthly SST
Chl−a
2010
2011
2012
2013

Figure 3

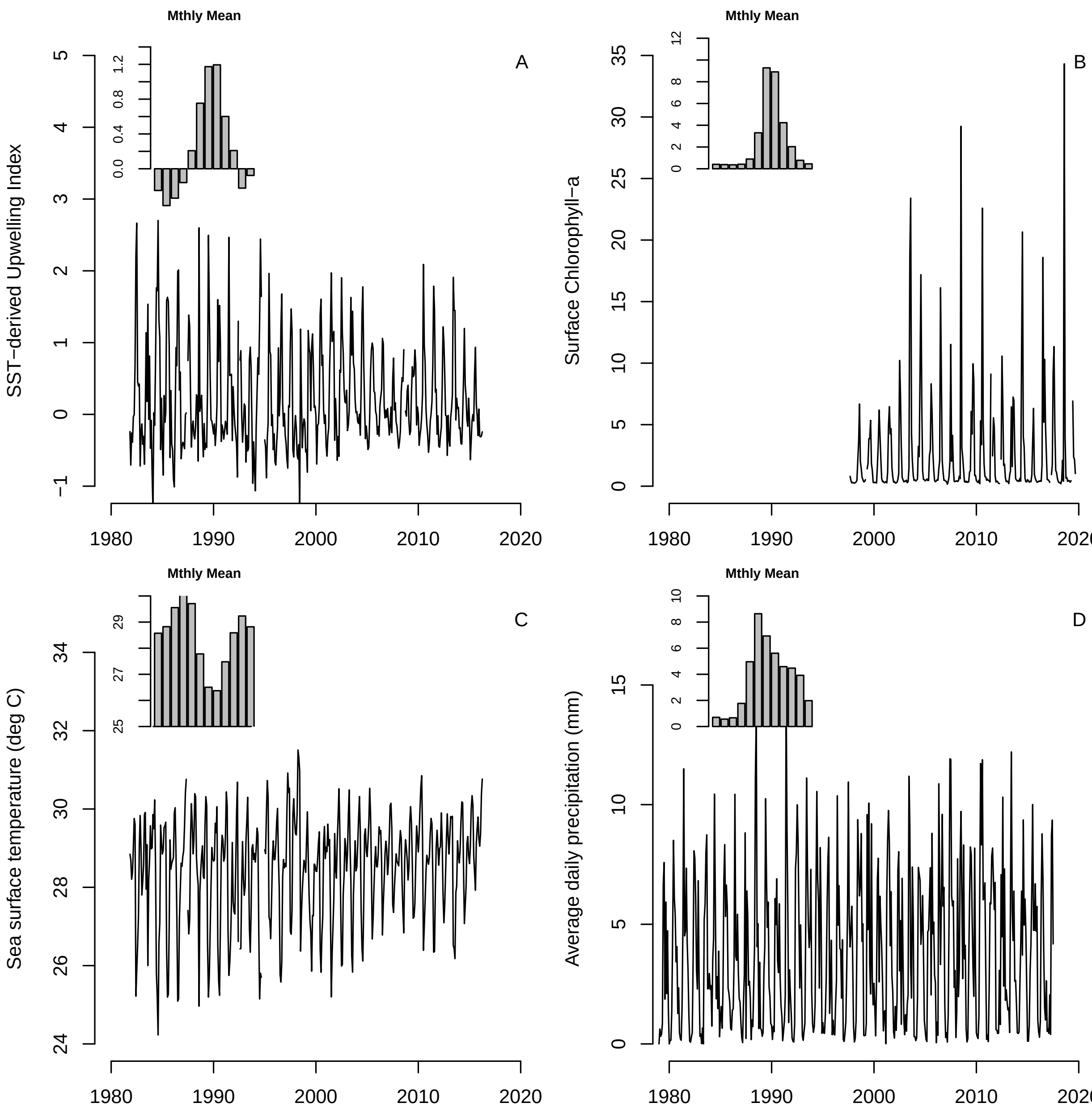
Mthly Mean
A
SST−derived Upwelling Index
Mthly Mean
B
Surface Chlorophyll−a
Mthly Mean
C
Sea surface temperature (deg C)
Mthly Mean
D
Average daily precipitation (mm)
1980
1990
2000
2010
2020

Figure 4

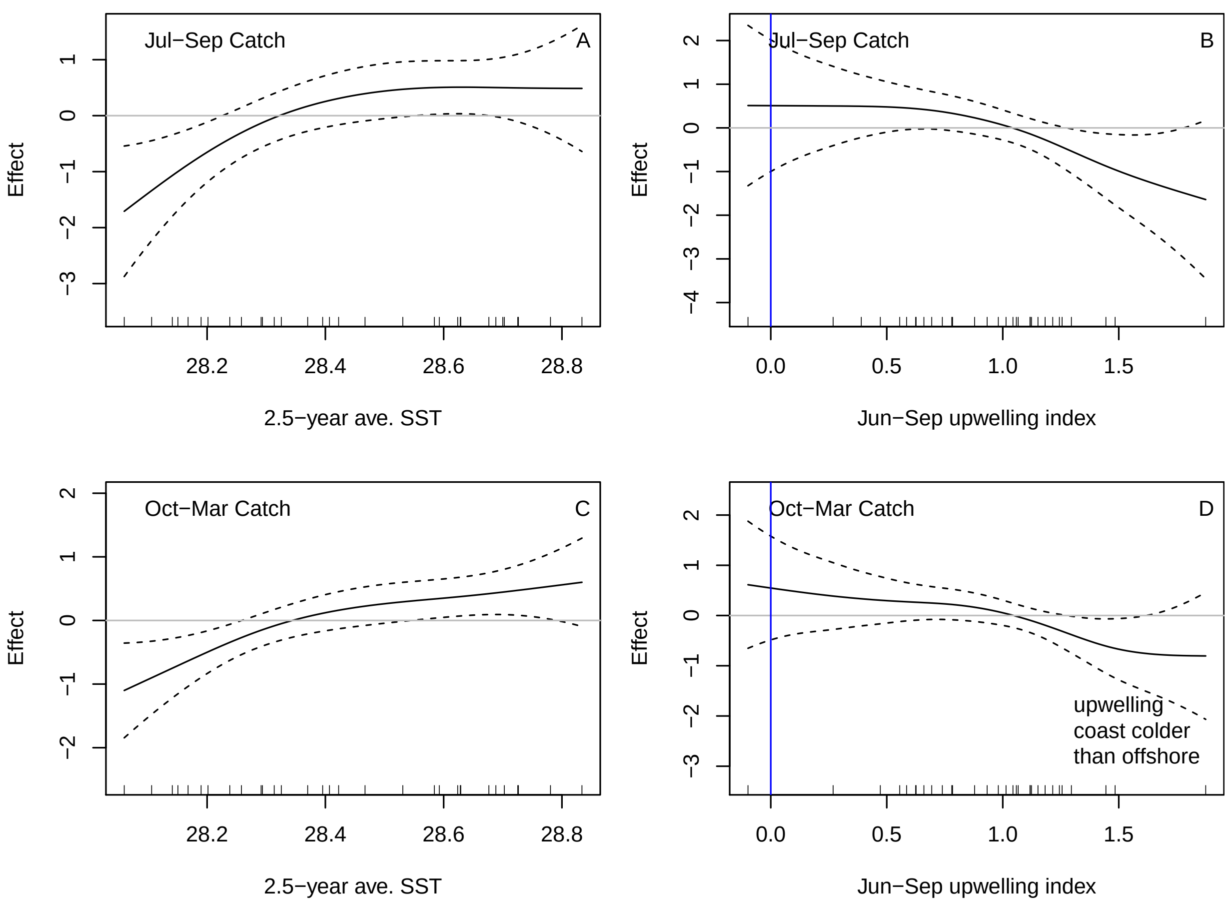

Jul−Sep Catch
A
Effect
2.5−year ave. SST
Jul−Sep Catch
B
Jun−Sep upwelling index
Oct−Mar Catch
C
Oct−Mar Catch
D
upwelling
coast colder
than offshore

Figure 5

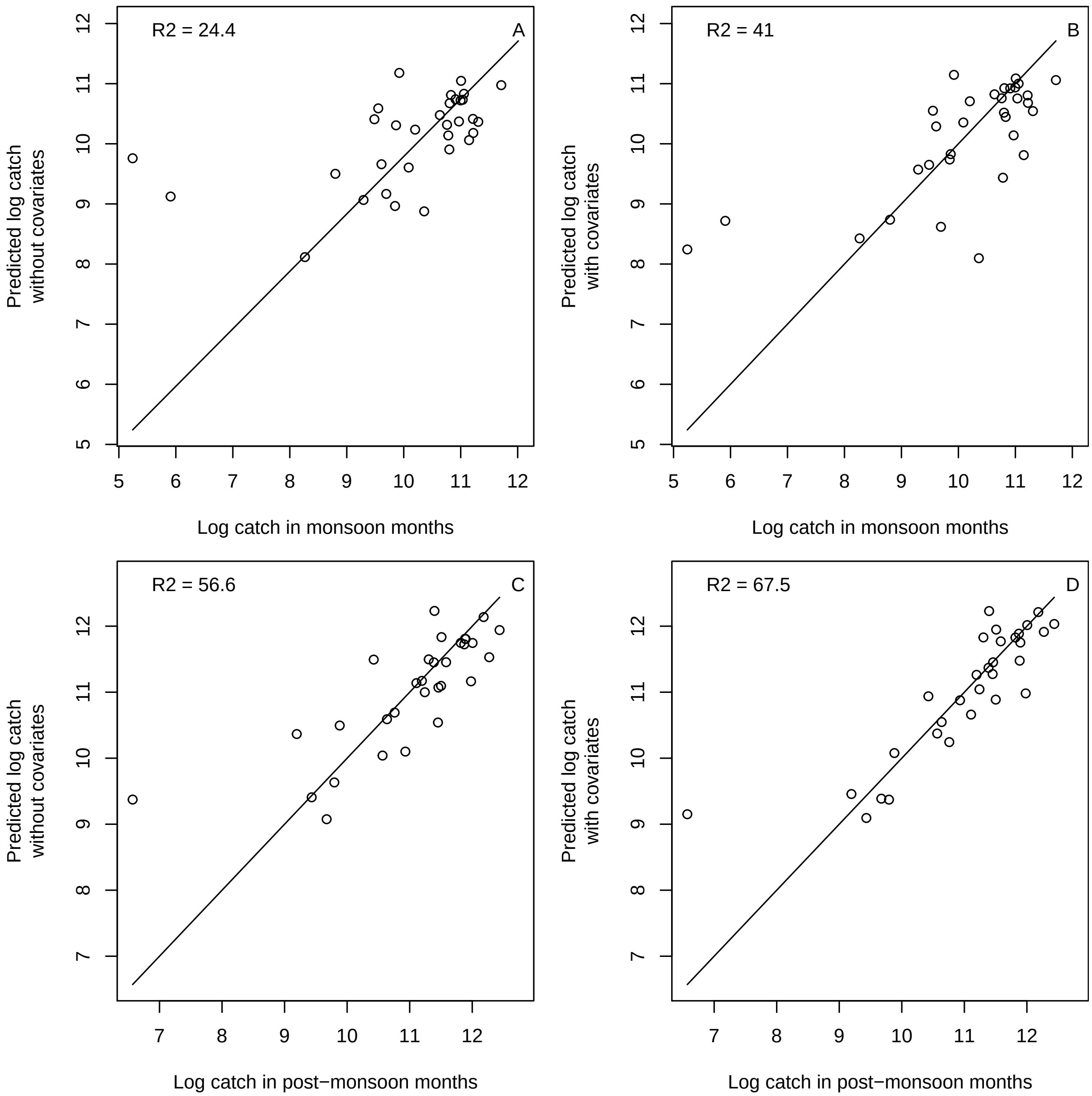

R2 = 24.4
A
Predicted log catch
without covariates
Log catch in monsoon months
R2 = 41
B
Predicted log catch
with covariates
Log catch in monsoon months
R2 = 56.6
C
Predicted log catch
without covariates
Log catch in post−monsoon months
R2 = 67.5
D
Predicted log catch
with covariates
Log catch in post−monsoon months

Figure 6